JACS
JOURNAL OF THE AMERICAN CHEMICAL SOCIETY
Article
pubs.acs.org/JACS

Alkenes as Alkyne Equivalents in Radical Cascades Terminated by Fragmentations: Overcoming Stereoelectronic Restrictions on Ring Expansions for the Preparation of Expanded Polyaromatics

Rana K. Mohamed,† Sayantan Mondal,† Brian Gold, Christopher J. Evoniuk, Tanmay Banerjee, Kenneth Hanson, and Igor V. Alabugin*

Florida State University, Tallahassee, Florida 32306, United States

Supporting Information

ABSTRACT: Chemoselective interaction of aromatic enynes with Bu_3Sn radicals can be harnessed for selective cascade transformations, yielding either Sn-substituted naphthalenes or Sn-indenes. Depending on the substitution at the alkene terminus, the initial regioselective 5-exo-trig cyclizations can be intercepted at the 5-exo stage via either hydrogen atom abstraction or C−S bond scission or allowed to proceed further to the formal 6-endo products via homoallylic ring expansion. Aromatization of the latter occurs via β-C−C bond scission, which is facilitated by 2c,3e through-bond interactions, a new stereoelectronic effect in radical chemistry. The combination of formal 6-endo-trig cyclization with stereoelectronically optimized fragmentation allows the use of alkenes as synthetic equivalents of alkynes and opens a convenient route to α-Sn-substituted naphthalenes, a unique launching platform for the preparation of extended polyaromatics.

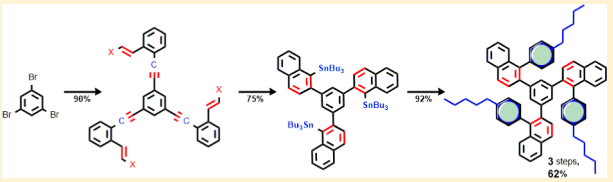

INTRODUCTION

Efficient synthetic routes to functional polyaromatic architectures[1] can be developed by leveraging the propensity of alkynes and oligoalkynes[2] to undergo cascade transformations into precisely shaped conjugated structures.[3,4] The two general approaches for transforming alkynes to polyaromatics utilize 6-exo or 6-endo cyclization of vinyl radicals in conjugated systems (Figure 1). The 6-exo approach is stereoelectronically favorable

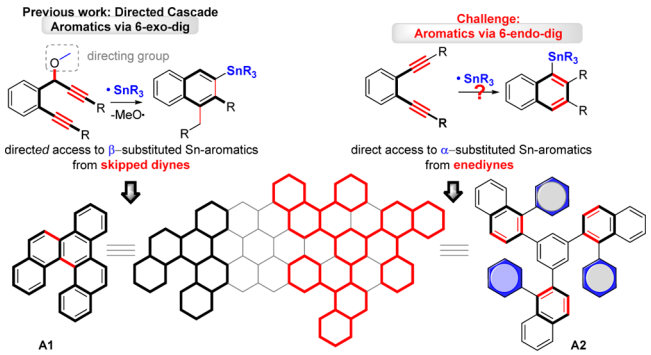

Figure 1. Potential approaches for achieving selectivity in radical cascades of oligoalkynes targeting extended polyaromatics.

and can be achieved in direct cascades of skipped oligoynes terminated by the elimination of a "traceless" directing group.[5] On the other hand, the radical 6-endo closure does not provide a reliable path to aromatic products,[6] and the development of efficient radical cyclizations with reliable selectivity continues to be a challenge.

In practice, the 5-exo/6-endo-dig competition is hard to control, and this approach often does not provide a satisfactory synthetic route to aromatic compounds.[7,8] Potentially, the yield of 6-endo products can be increased by "recycling" 5-exo products via homoallylic ring expansion, as described in Figure 2. However, such expansion is impossible for the vinyl radicals derived from alkynes. As a result, the Bu_3Sn-mediated radical cyclization of enediynes exclusively forms the 5-exo-dig benzofulvene products.[9,10]

The key difference between alkenes and alkynes in the 5-exo → 6-endo ring expansion is stereoelectronic. In the case of

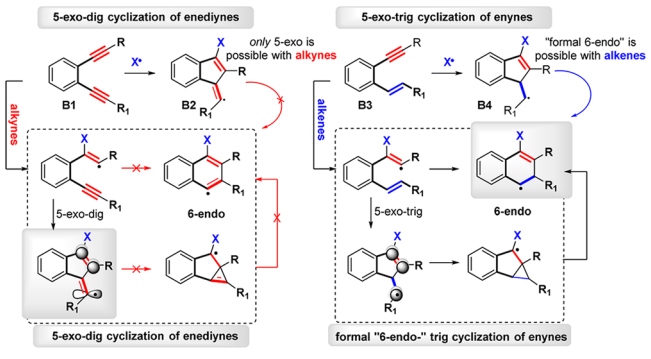

Figure 2. Left: Stereoelectronic restriction on the 5-exo-dig → 6-endo-dig homoallylic ring expansion. Right: "Recycling" of 5-exo-trig products into 6-endo-trig products via homoallylic ring expansion is stereoelectronically feasible.

Received: March 5, 2015
Published: April 23, 2015

DOI: 10.1021/jacs.5b02373
J. Am. Chem. Soc. 2015, 137, 6335−6349

enediynes, the favored 5-exo-dig cyclization produces a vinyl radical that is constrained orthogonally to the endocyclic π-system (Figure 2, left). In contrast, the 5-exo-trig cyclization of enynes forms a flexible alkyl radical that *can* rearrange into the formal 6-endo product via the *homoallylic ring expansion* sequence (Figure 2, right). Due to the absence of stereoelectronic limitations, the ring expansion of 5-exo-trig products is well-documented.[11,12]

Earlier, we disclosed a strategy for chemo- and regioselective reactions of aromatic enynes with Bu_3Sn radicals, leading to the formation of indenes or dienes.[13] In a subsequent communication, we reported that proper substitution at the pendant alkene allows the formation of the six-membered products. Formal oxidation of the 6-endo products to fully aromatized naphthalene derivatives can be achieved by incorporating a "self-terminating" C−C bond β-scission as the final step of the cascade.[14] The combination of cyclization and fragmentation allows the use of alkenes as synthetic equivalents to alkynes by overcoming stereoelectronic restrictions imposed by the rigidity of vinyl radicals.

Herein, we provide full experimental and computational analysis of this new process and apply it toward the construction of a diverse library of α-Sn β-substituted naphthalene building blocks with the aim to develop a convenient strategy for the synthesis of large polycyclic aromatic hydrocarbons such as 1,3,5-tris(naphthyl)benzenes (**A2**, Figure 1) and other extended derivatives. We outline the scope and limitations of this strategy and show that this C−C bond fragmentation, accomplished through the rational design of radical leaving groups on the alkene, serves as a formal "oxidation" step needed for the crossover between the products of alkene and alkyne cyclization. The fragmentation is fast due to selective transition state (TS) stabilization originating from a through-bond (TB) interaction between a radical center and a lone pair at the δ-atom, a new electronic effect in radical chemistry. Furthermore, we identify a 1,2-stannyl shift as a new mechanism for equilibration between two vinyl radicals with potential implications for the use of dynamic covalent chemistry (DCC) in radical reactions.

COMPUTATIONAL METHODS

All calculations were performed using the Gaussian 09 program package.[15] Unless otherwise noted, the M06-2X/LanL2DZ[16] was used to evaluate the stationary states at the radical potential energy surfaces. The M06-2X method accounts for dispersion using a reparameterized exchange−correlation functional and is substantially less computationally demanding than multiconfigurational methods. Frequency calculations were performed to confirm each stationary point as either a minimum or a first-order saddle point. Nucleus independent chemical shift values (NICS(0) and NICS(1))[17] were obtained using the gauge-including atomic orbital (GIAO) method[18] at the M06-2X/LanL2DZ level of theory. Chemcraft 1.7[19] and CYLView[20] were used to render the molecules and orbitals. The NBO 3.0 program was used to analyze electronic properties of reactive intermediates.[21] For the majority of the computations, unless otherwise stated, we used a truncated Me_3Sn radical instead of the bulkier Bu_3Sn radical utilized in the experimental work in order to alleviate computational challenges arising from the presence of multiple conformations in the three Bu groups of Bu_3Sn.

RESULTS AND DISCUSSION

While investigating the scope of enyne radical cyclizations, we found that, despite the presence of four possible locations for intermolecular radical attack, all observed products result from Bu_3Sn radical addition to the internal alkyne atom. Furthermore, this chemoselective attack leads to subsequent cyclizations with remarkable regio- and stereoselectivity. Such selectivity warrants a more extensive discussion.

In radical chemistry, organotin hydrides are so versatile that their ubiquity has been deemed the "tyranny of tin".[22] Tin hydrides are popular reagents for reductive additions to alkenes and alkynes with utility extending to inducing selective cyclizations, complex rearrangements, and domino (cascade) reactions.[23] In particular, intermolecular radical addition to alkynes opens access to reactive vinyl radicals that can participate in reaction cascades.[24] A number of literature reports, a few of which are summarized in Scheme 1, suggest

Scheme 1. Sn-Mediated Radical Cyclizations of Enynes from the Literature

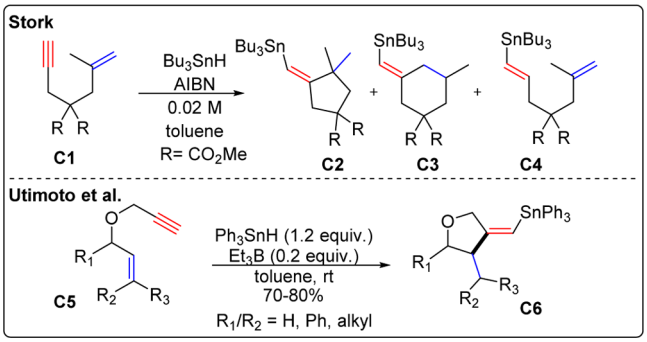

that, in multifunctional systems, Sn radical addition to *terminal* alkynes is preferred over reaction with an alkene.[25−27] Overall, selective addition in these systems proceeds in a Markovnikov fashion to form the more stable vinyl radical. However, the present case (enyne) corresponds to attack at an *internal* alkyne. Furthermore, the attack occurs at the *internal carbon of the alkyne*, forming the less conjugated and *less stable* of the two vinyl radicals.

To gain further insight into the relative reactivity of disubstituted alkynes and alkenes toward Bu_3Sn radicals, we performed competition experiments in which an equimolar mixture of *trans*-stilbene and tolane reacted with 1.0 equiv of Bu_3SnH (in the presence of 0.2 equiv of azobisisobutyronitrile (AIBN), Scheme 2). The results were interesting—we observed highly selective addition to the alkyne with the alkene recovered in the unreacted state.[28]

Scheme 2. Competition Experiment with Tolane and *trans*-Stilbene

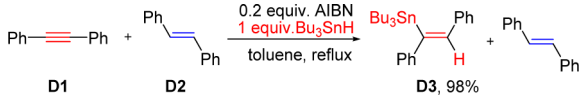

Stage 1: Dynamic Covalent Chemistry. Computations provided deeper insights into the origin of the observed reaction selectivity and the possible involvement of a pool of equilibrating radicals self-sorted via their relative reactivity or stability.[29] In an extreme situation, such a system can be considered to be an example of DCC[30−32] in radical transformations. In this scenario, the system can take advantage of the feasibility of "error-checking" in DCC when fast equilibration allows covalent bonds to reversibly form, break,

DOI: 10.1021/jacs.5b02373
J. Am. Chem. Soc. 2015, 137, 6335−6349

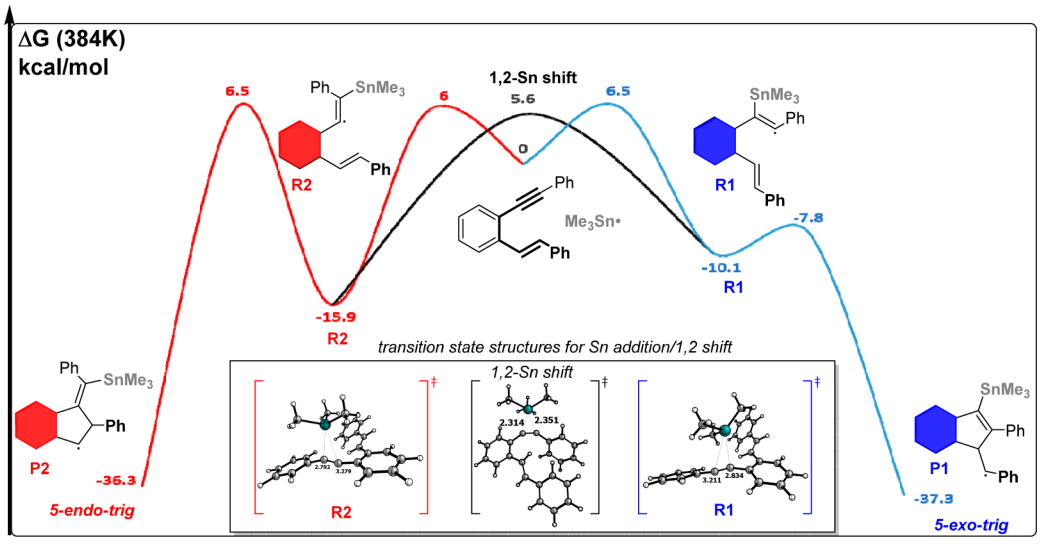

Figure 3. Potential energy surface for the formation, interconversion, and cyclization of two vinyl radicals at the M06-2X/LanL2DZ level of theory. Single-point solvation corrections on gas phase geometries (PCM, toluene) are given in the Supporting Information.

and re-form to ultimately afford *one* out of several possible products. In the present work, we consider only a subset of such reactions that originate from the Bu_3Sn attack on the alkyne. This simplification is made possible by the observed experimental selectivity presented in Scheme 2. On the basis of these experimental findings, we concentrated our computational analysis on reaction pathways originating from addition of the Bu_3Sn radical to the alkyne moiety of enynes.

In order to understand the possible equilibria between the two vinyl radicals, we performed M06-2X/LanL2DZ evaluation of the two transition states for the Me_3Sn radical addition to the alkyne moiety of the enyne. According to the principle of microscopic reversibility, the same transition states correspond to β-scission of the two radicals to give back the staring materials. Additionally, we have located the transition state for the 1,2-Sn shift that provides a direct way to interconvert the two vinyl radicals. We also evaluated the barrier and reaction energies for the subsequent cyclization pathways that led to the formation of five-membered products (Figure 3).

Unique Features of Sn Radicals. Computations also highlighted the unique properties of Sn reagents relative to other radical sources (Figure 4). Most importantly, the addition of a Sn radical to tolane had the smallest thermodynamic driving force and is closer to being thermoneutral than the analogous addition of CMe_3 and $SiMe_3$ radicals to the same alkyne. Furthermore, the barrier for Sn addition is relatively low. Together with the low exergonicity, this feature makes the β-scission barrier relatively low, as well (~18 kcal/mol at the chosen levels of theory).

An interesting possible explanation for the unusual computational trends is the greater strength of hyperconjugative interactions between the developing radical center and the C−Sn bond (Table 1).[33] The importance of hyperconjugation is apparent from the calculated energies of addition which do not follow the order of the literature bond dissociation energies (BDEs): C−C (~90) > C−Si (~89) > C−Sn (~70).[34] For instance, addition of the $SiMe_3$ radical is favored by >10 kcal/mol relative to the *t*-Bu radical, despite having nearly identical BDEs. In a similar way, the calculated difference in reaction energies between $SnMe_3$ and the *t*-Bu radical (<5 kcal/mol) is much smaller than the large difference in BDEs (~20 kcal/

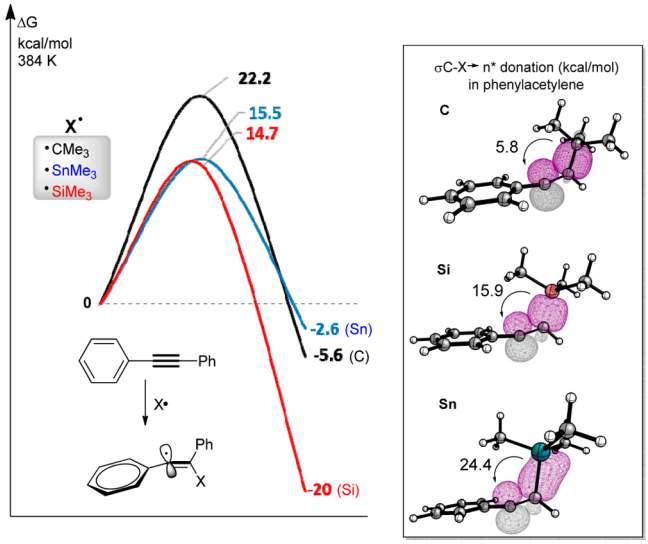

Figure 4. Left: Values for the addition of XMe_3 radicals to tolane calculated at the M06-2X/LanL2DZ level of theory. Right: Comparison of hyperconjugative $\sigma_{C-X} \rightarrow n^*$ stabilizing interactions (β-spin orbitals) for the vinyl radicals formed upon addition of XMe_3 radicals to phenylacetylene.

mol). Significant hyperconjugative stabilization of the radical center by the $SiMe_3$ and $SnMe_3$ groups provides a plausible explanation to these observations. Furthermore, the lower barriers for addition of $SnMe_3$ radicals suggest that such effects start to manifest themselves in the TS.[35]

Furthermore, hyperconjugative interactions are stronger in the more sterically crowded systems where a smaller CCX angle is imposed by additional substitution (i.e., 115° vs 119° angles for the radicals formed by Sn addition to phenylacetylene and tolane). As a result of these geometric changes, the carbon hybrid in the C−Sn bond gains more p-character (increases from 70−73 to 75−78%), making this bond a better partner in stabilizing hyperconjugative interactions (Figure 5).[36,37] This observation highlights the importance of sterics in Sn additions and provides a possible explanation for the greater

DOI: 10.1021/jacs.5b02373
J. Am. Chem. Soc. 2015, 137, 6335−6349

Table 1. Optimizing Conditions for the Radical Cyclization of Enynes

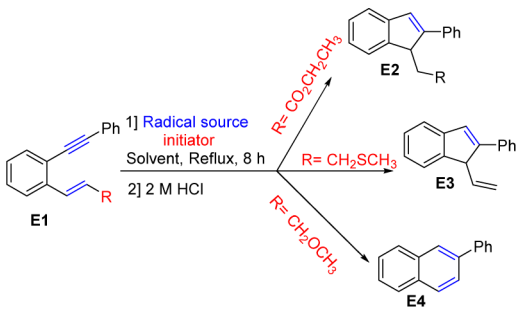

ENTRY	•R Source 1.2 equiv.	Initiator 0.5 equiv.	Solvent	Yield % [E4]	[E2][a]
1	Bu_3SnH	AIBN	Benzene	12	40
2	Bu_3SnH	AIBN	Acetonitrile	26	24
3	**Bu_3SnH**	**AIBN**	**Toluene**	**75**	**87**
4	$(Me_3Si)_3SiH$	AIBN	Toluene	SM[b]	SM[c]
5	Et_3SiH	AIBN	Toluene	NR	NR
6	Ph_3SnH	AIBN	Toluene	24	20
7	Bu_3SnH	DTBPB	Toluene	44	52
8	Bu_3SnH	TOOT	Toluene	65	18
9	Bu_3SnH	ABCN	Toluene	51	60

[a]Usingn 0.4 equiv of initiator. [b]Starting material decomposed. [c]Complex mixture.

exothermicity and lower barriers for the radical additions to the enyne in comparison to that in tolane.

Stage 2: Kinetic Self-Sorting. The presently available accuracy of density functional theory computations should be taken as semiquantitative, and we treat these results as preliminary, but the computations suggest a very interesting picture. In particular, the analysis reveals that the experimentally observed dominating pathway is derived from the less stable of the two vinyl radicals. Furthermore, the reactive radical is also formed from the parent enyne via a higher addition barrier. This seemingly surprising result is due to an imbalance induced in the dynamic equilibria between the two radicals via fast and irreversible 5-exo-trig cyclization. This form of "kinetic self-sorting" leads to high selectivity, an otherwise unlikely outcome.

Formation of the more stable "internal" radical **R2** in Figure 6 is unproductive because its cyclizations are stereoelectronically disfavored by the necessity to lose benzylic conjugation with the central aromatic ring before reaching the cyclization TS. Due to the high barrier (>22 kcal/mol) for the cyclization of radical **R2**, its formation cannot lead to a cyclized product and would be a dead end if not for the possibility of conversion to the "productive" radical **R1**. Computations suggest two mechanisms for interconversion between the two radicals. First, the radical can revert back to the starting materials via β-scission of the Sn−C bond. At the present level of theory, the Curtin−Hammett principle suggests that equilibration of the two radicals via β-scission is less energetically likely since the absolute value of the free energy for the activation barrier for the formation of radical **R1** is ∼1 kcal higher than that for the 5-endo cyclization of radical **R2**. One has to keep in mind, however, that the 1 kcal/mol difference may well be within the computational uncertainty of the presently available computational methods.

Second, computations identified a new mechanism for the interconversion based on a 1,2-stannyl shift. This shift was found to have a barrier of only 5.6 kcal/mol, providing a more likely direct explanation for the observed selectivity. It was suggested that, due to its large size and the availability of low-lying empty 5d atomic orbitals, tin can expand its valence to facilitate metallotropic shifts (intramolecular migration).[38] Fast [1,5]-Sn shifts[39] in cycloheptatrienyl tin compounds as well as [1,9]-Sn shifts in cyclononatetraenyl tin compounds[40] have been reported (Figure 7). The barrier for the 1,5-shift of $SnMe_3$ in cyclopentadiene had been calculated to be 8.4 kcal/mol,[41] significantly lower than the 27 kcal/mol barrier reported for the analogous 1,5-H shift.[42]

The importance of the R_3Sn group for the initiation of these reactions is clearly evidenced by the experimental screening of enynes with a variety of initiators and radical reagents, as shown in Table 1. The combination of Bu_3SnH and AIBN in refluxing toluene was the most efficient for inducing cyclizations.

Stage 3: Transformations of the Initially Formed 5-exo-trig Radicals. To test the scope of this reaction, a variety of enynes were synthesized using strategies based on sequential Wittig reaction and Sonogashira coupling (see Supporting Information for details). The outcome of cyclizations depended strongly on the nature of substitution at the alkene terminus. The presence of radical-stabilizing groups led to the clean formation of the 5-exo-trig products (indenes), whereas alkyl groups directed the process toward the formation of 6-endo products (Figure 8). The nature of these substituent effects and the hidden complexity of the reaction mechanism are discussed in the following sections.

Formation of Indenes. Under the optimized conditions, when the alkene substituent R is CO_2Et and the alkyne substituent is Ph, indene **F11** was the sole product obtained in 87% yield as a result of 5-exo-trig cyclization, followed by rapid hydrogen atom abstraction (HAA). The scope of this reaction

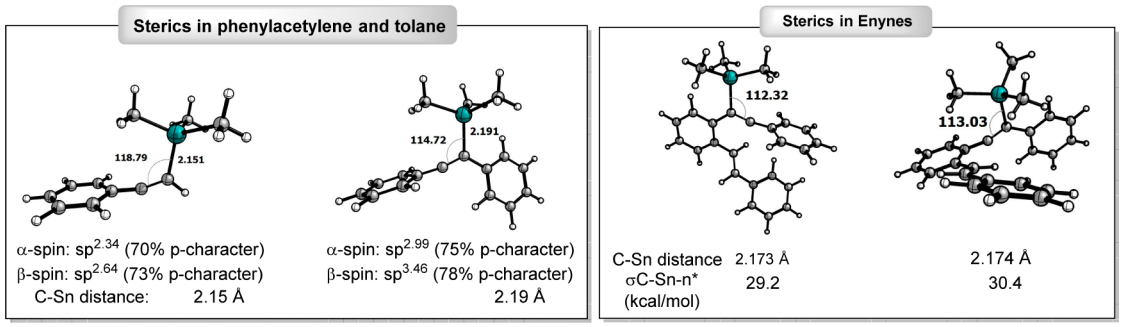

Figure 5. Steric congestion from larger substituents imposes a smaller CCSn angle, and the resulting increase in p-character (and donor abilities) of the C−Sn bond enhances hyperconjugative interactions.

DOI: 10.1021/jacs.5b02373
J. Am. Chem. Soc. 2015, 137, 6335−6349

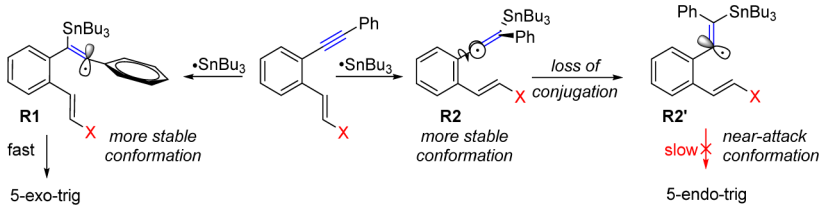

Figure 6. Loss of conjugation needed to reach the near-attack conformation disfavors cyclization of **R2**.

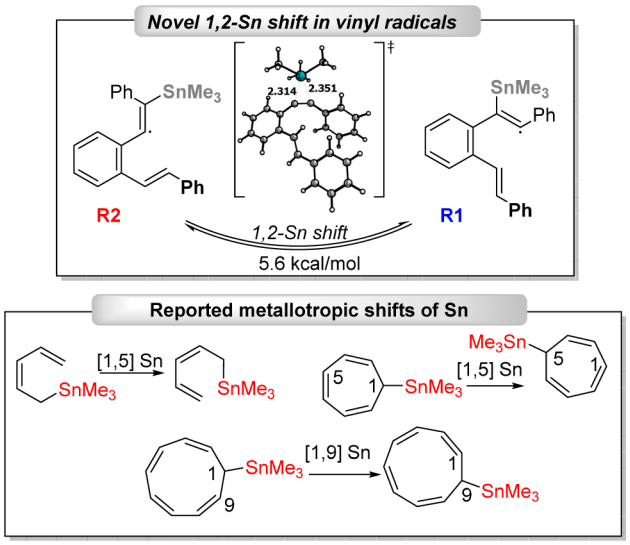

Figure 7. Top: Computations identified a low-barrier (5.6 kcal/mol) mechanism for the interconversion of vinyl radicals **R1** and **R2** based on a novel 1,2-stannyl shift. Bottom: Labile nature of the C−Sn bond suggested by 1,5- and 1,9-sigmatropic Sn shifts reported in the literature.

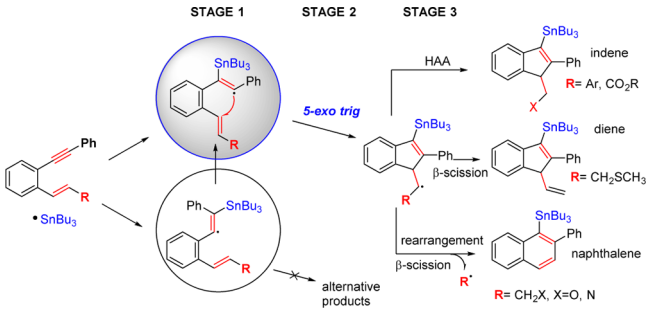

Figure 8. Suggested origin of selectivity and control of propagation of enyne radical cascade via alkene substituents.

is demonstrated by the successful transformation of a variety of enynes into the library of indenes shown in Figure 9. For the radical-stabilizing substituents (i.e., X = ester or Ph), the radical product of 5-exo cyclization is always intercepted by HAA to form indenes. Indene formation is particularly efficient with electron-rich substrates at the alkyne terminus. Alkyl and tetramethylsilane-substituted alkynes also gave good yields but required longer reaction times. The reaction retained its efficiency when the alkene substitution was changed from ester to amide, cyano, and substituted aryl groups (compounds **F18**−**F20**).

Switch to "endo" Selectivity. A dramatic change in selectivity was observed in the absence of radical-stabilizing groups at the alkene terminus (Scheme 3). Under the

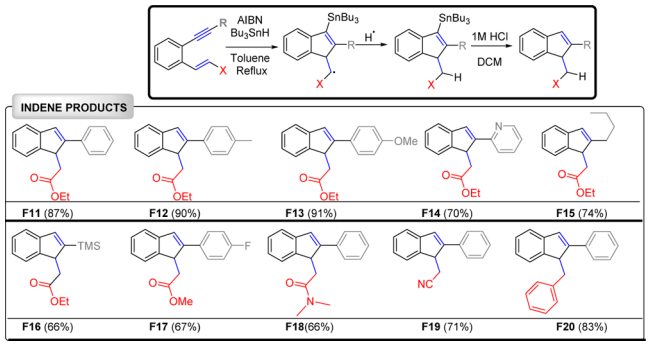

Figure 9. Library of indenes accessed via 5-exo-trig cyclization of aromatic enynes.

Scheme 3. Change in Selectivity Observed upon Altering Substitution at the Alkene Terminus

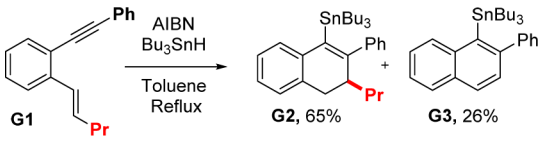

optimized conditions discussed above, the alkyl-substituted enyne **G1** gave a mixture of two six-membered products, **G2** (65%) and **G3** (26%): the major one corresponded to the 6-endo-trig product terminated by HAA, whereas the minor one originated from C−C bond fragmentation in the cyclic product.

Cyclization/Ring Expansion Sequence. The observed switch in selectivity could have two alternative origins. In the first scenario, the switch in substitution could change kinetic preferences for the cyclization, rendering the 6-endo step faster. In the second possible scenario, the cyclization would proceed via a 5-exo-trig path followed by a ring expansion process (Scheme 4).

Experimental Evidence for the 5-exo/Ring Expansion Sequence. In the case where X = CH_2SEt, rapid C−S bond scission intercepted the cascade after 5-exo-trig cyclization, producing dienes **I2** and **I3** after isomerization, as shown in Scheme 5. The high efficiency of this bond scission illustrates that this process can be conveniently used as a "radical clock" for the experimental study of radical reaction mechanisms. The fragmented thiyl radical is relatively reactive and likely assists in the isomerization of the initially formed nonconjugated diene into two conjugated diene products, the majority of which is derived from HAA at the benzylic position.[43] A small amount (~4%) of the naphthalene product **I4** was also observed. Subsequent computational analysis suggested that the minor product **I4** could have been derived directly via the 6-endo-trig pathway due to the smaller $\Delta G^{\ddagger}$ difference between 5-exo and 6-endo pathways for this substrate (0.6 kcal/mol).

The interception of the intermediate 5-exo-trig product via β-scission of the weak C−S bond provided direct mechanistic

DOI: 10.1021/jacs.5b02373
J. Am. Chem. Soc. 2015, 137, 6335−6349

Scheme 4. Six-Membered Products Can Form Either via Direct 6-endo-trig Products or via a Sequence of 5-exo-trig/3-exo-trig Cyclizations Followed by C−C Bond Scission

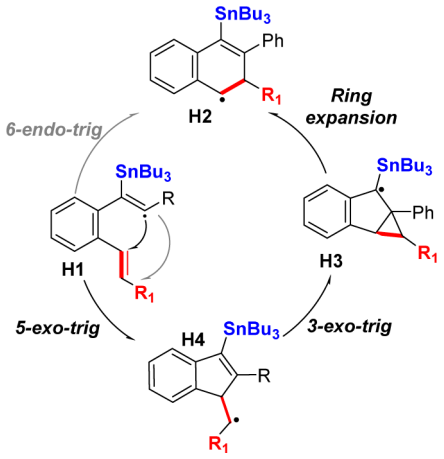

Scheme 5. Presence of a Weak C−S Bond Allows Trapping of the Initial 5-exo-trig Product via C−S Scission and Prevents the Homoallylic Ring Expansion into Naphthalene

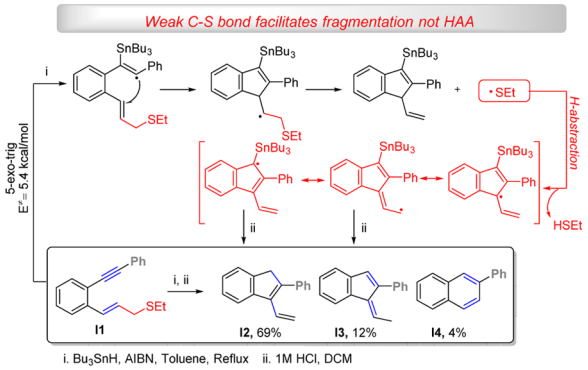

evidence that, even after the alkene substituent was altered from a radical-stabilizing group (Ar, ester) to an alkyl group, the cyclization preferentially proceeded via the 5-exo path. We will provide computational comparison of the direct 6-endo path and the 5-exo/3-exo/fragmentation cascade in one of the following sections. However, first, we will discuss experimental data for the final step of the cascade, the aromatization of naphthalenes via scission of an exocyclic C−C bond.

Terminating the Ring Expansion via Fragmentation: Rational Design of Radical Leaving Groups. The feasibility of the fragmentation pathway is largely rationalized by the aromatic stabilization gained in the conversion of the initial 6-endo-trig products into naphthalenes. The fragmentation is further enhanced by stabilizing the departing radical fragment via the rational design of radical leaving groups. A balance between stability and reactivity is crucial because the reactivity of radicals formed in fragmentations dictates the outcome of the competition between propagation and termination of radical cascades. In particular, reactive radicals can react further in an undesirable way. We aimed to design the cascade such that the balance between stability and reactivity is struck, resulting in the sole formation of naphthalenes. We found that this is possible upon altering the alkene substituent to CH_2XCH_3, where X = O or NMe (Figure 10).

The 2-center, 3-electron (2c-3e) delocalization between the alkyl radical center and lone pair of the adjacent heteroatom

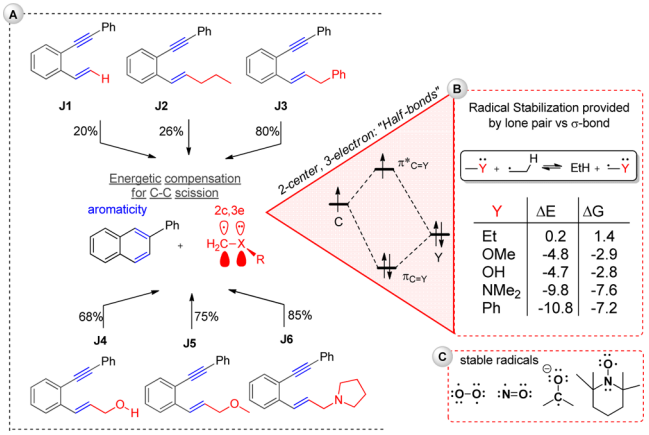

Figure 10. (A) Efficiency of fragmentation can be increased by proper substitution at the alkene terminus. (B) 2-Center, 3-electron interactions are stabilizing "half-bonds" that account for radical stabilization energies in heteroatom-substituted radicals (at the UM062X/LanL2DZ level). (C) Important molecules stabilized by 2c−3e bonds.

serves to stabilize the radical leaving group effectively allowing the cascade to "self-terminate". This term was introduced by Wille et al. to describe transformations[44] where stable fragmenting radicals "exit" the reaction without exhibiting subsequent reactivity.[45] Such 2c-3e interactions correspond to the formal bond order of 1/2 and can be referred to as "half-bonds". Their presence accounts for the observed increase in the yield of naphthalenes from enynes, incorporating this rational design. Figure 10 shows substrates containing either Ph or a heteroatom at the pendant alkene. For both substitution patterns, the fragmentation/aromatization proceeds fully because both the Ph group and the lone pairs are better radical-stabilizing substituents than C−H/C−C bonds.[46] Furthermore, the higher product yield for X = N relative to X = O is consistent with nitrogen being a better donor than oxygen.[47] As expected, an increase in the experimental yields correlates with greater reaction exergonicity: CH_2NMe_2 > CH_2OMe/CH_2OH > CH_2alkyl (Figure 10). Elimination of a benzylic radical (R = CH_2Ph) is also a viable, albeit less atom-economical, option.

Coupling Ring Expansion to Fragmentations: From Enynes to Naphthalenes. All enynes in Figure 11 cyclized to the substituted naphthalenes selectively and, with a few exceptions, in very good yields. The variations of substituents at the alkyne terminus demonstrated that the reaction's efficiency increased when substituents on the alkyne terminus provided additional delocalization to the vinyl radical formed via the initial intermolecular attack (Figure 11, **K23**−**K25**). The reaction retained its efficiency when alkene substitution was changed from hydrogen to a methyl group and became more efficient with the methyl substituent on the inner alkene carbon (Figure 11, **K20**).

Limitations. Alkyne substitution plays a crucial role in the formation of the right initial radical. In order for the cyclization to work, the Bu_3Sn attack has to occur at the "internal" alkyne carbon. The two examples in Scheme 6 illustrate this point as well as the interesting observation that formation of naphthalenes seems to be more sensitive to substitution at the alkyne terminus than formation of indenes. For example, the dialkyl enyne **L1** does not give a cyclic product, whereas the respective alkyl ester **L1′** provides 74% of the indene. These

DOI: 10.1021/jacs.5b02373
J. Am. Chem. Soc. 2015, 137, 6335−6349

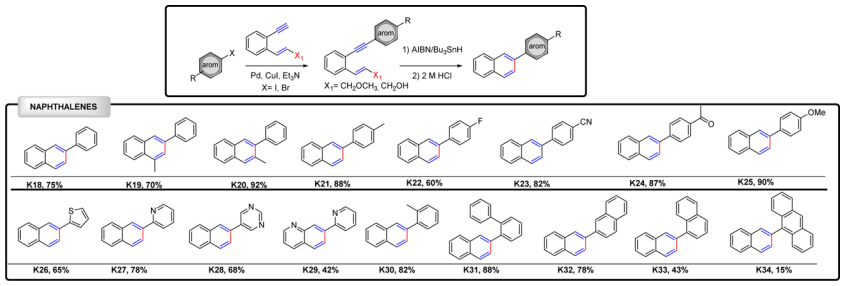

Figure 11. Formation of naphthalene products upon cyclization of aromatic enynes with suitable alkene substitution.

Scheme 6. (Top) Limitations in the Bu_3Sn-Mediated Radical Cyclization of Enynes When Electronic Factors Disfavor Reactions of Radical B and (Bottom) Low Yield of L8 and Formation of L9 Showing How Steric Congestion in the Naphthyl-Substituted Enyne Decreases the Efficiency of Cyclization

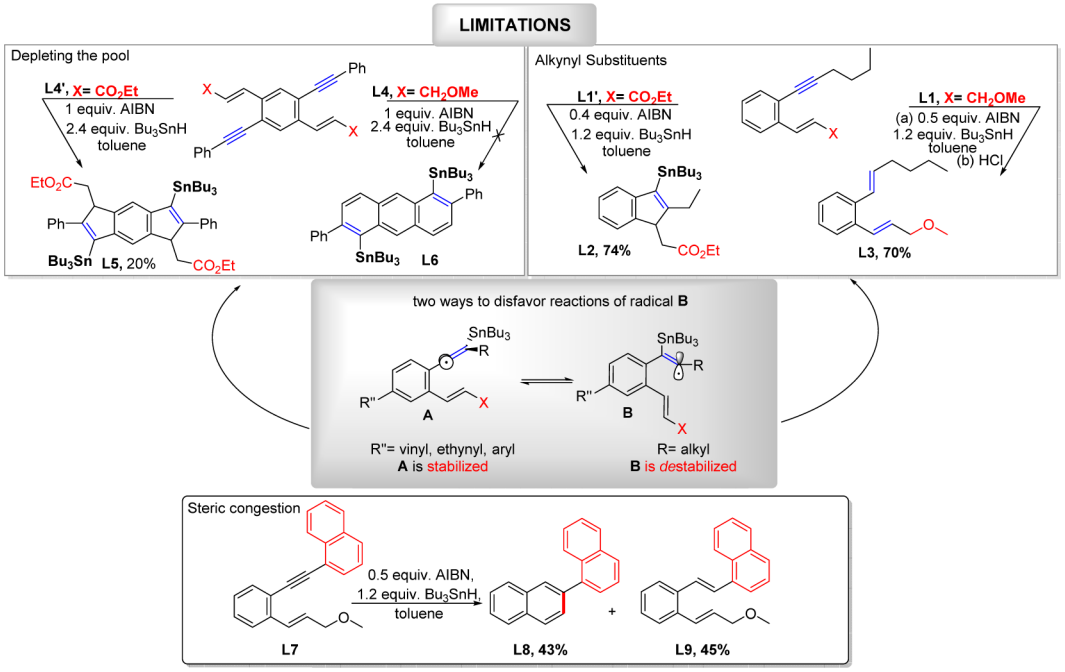

results suggest that the alkyl-substituted vinyl radical is too unstable to be present in sufficient amounts for the cyclization, especially if this cyclization has to involve an intramolecular attack at a nonactivated (alkyl-substituted) double bond. The potential 5-endo/4-exo-trig cyclizations of the alternative vinyl radical are known to be relatively inefficient, so the benzylic radical has no choice but to abstract hydrogen and form the reduced acyclic product.

Stabilization of the internal vinyl radical A (Scheme 6) by conjugation provides an alternative way to deplete the reactive radical pool, as illustrated by the lack of anthracene product from the bisenyne **L4**. Again, intramolecular attack at the activated alkene (X = CO_2Et) does not suffer from this as much as attack at the nonactivated alkene (X^- = CH_2OMe). Furthermore, the cyclization can be disfavored by sterics, resulting in the formation of acyclic reduced products as is the case for the naphthyl-substituted enyne **L7**.

Mechanistic Insights into the Fragmentation Step. Intramolecular trapping of the benzylic radical with a pendant alkene using enyne **M1** was unsuccessful and indicated that β-scission is sufficiently fast to compete with 6-exo cyclization (Scheme 7A). The stabilized CH_2XR radical formed in the fragmentation step is unreactive to sensitive functionalities, that is, to the alkyne and alkene moieties in enyne reactants and to the polyaromatics formed. To circumvent the volatile nature of

Scheme 7. Attempts To Trap and/or Isolate Products Associated with the Departing Radical Fragment

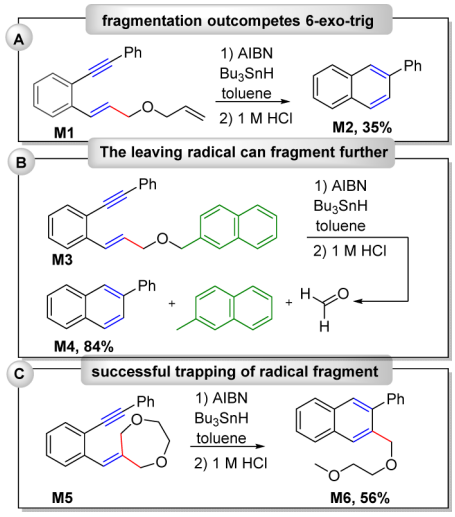

DOI: 10.1021/jacs.5b02373
J. Am. Chem. Soc. 2015, 137, 6335−6349

the fragment, enyne **M3** was synthesized; although successful cyclization to naphthalene was evident, the reaction mixture indicated that the α-oxy alkyl radical fragmented further into the β-methyl naphthalene product shown in Scheme 7B. Ultimately, successful "trapping" of the radical fragment was accomplished in the cyclization of spiroalkene **M5**, where the fragmenting radical remained attached to the substrate **M6** (Scheme 7C).

Possible Ring Expansion Mechanisms. Further experiments were carried out with the goal of delineating the ring expansion cascade and differentiating between the two possible routes (Scheme 8).

Scheme 8. Lack of Carbon Transposition of the Substituted Alkene Rules out the Neophyl Pathway as the Rearrangement Mechanism

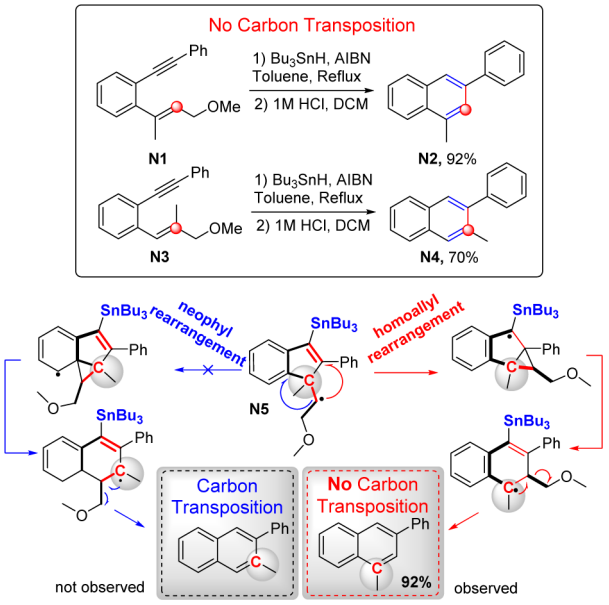

As shown in Scheme 8, the intramolecular rearrangement of the 5-exo radical adduct into the formal 6-endo benzylic radical occurs via 3-exo-trig attack at the "isolated" double bond as a homoallyl ring expansion (red pathway, Scheme 8) rather than at the vicinal benzene ring as a neophyl ring expansion (blue pathway, Scheme 8). This is experimentally supported by the lack of carbon transposition product observed upon the cyclization of enyne **N1**. Both the neophyl and the homoallyl ring[48] openings are exergonic (~16 and ~12 kcal/mol relative to the 5-exo radical)[14] as expected for the less-strained six-membered radical, which is significantly stabilized by additional electronic effects (i.e., allylic and benzylic resonance). However, the barrier for the 3-exo closure onto the "isolated" alkene is much lower than the barrier for cyclization that disrupts aromaticity, although the former barrier is still quite significant due to accumulation of strain in the tricyclic moiety.

The need to use a stoichiometric amount of initiator (0.5 equiv of AIBN produces 1 equiv of isobutyronitrile radical) for full conversion to naphthalene further suggested the "self-terminating" nature of the cascade via β-C−C bond scission. In other words, the fragmented radicals did not efficiently propagate the radical chain process. The absence of significant amounts of acyclic products suggested that premature HAA from R_3Sn-H by the acyclic radicals could be controlled by concentration of reagents. Slow addition of Sn kept its concentration low at any given time and allowed sufficiently fast intramolecular reactions, especially 5-exo-trig, to dominate the reaction pathway.

Computational Analysis of the Full Cascades. Questions still remained regarding the interplay of effects dictating product selectivity. Computations and experiments elucidated the multifold role of the pendant alkene in the transformation to naphthalene and further supported the intermediacy of the 5-exo step. In particular, the computational analysis found a significantly higher activation barrier for 6-endo-trig ring closure relative to the alternative 5-exo-trig cyclization. Even for the alkene with the CH_2OMe substituent, where the 5-exo product does not get additional stabilization through

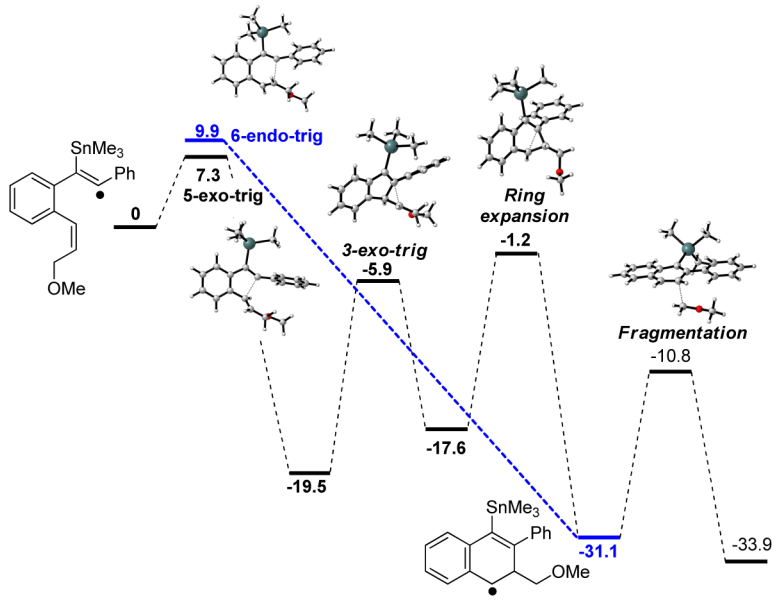

Figure 12. Calculated free energy profile for the alternative paths to 6-endo-trig products: Sn-mediated cyclization/ring expansion (black) vs direct 6-endo-trig (blue) at the UM062X/LanL2DZ level of theory. ΔG values, in kcal/mol, are calculated at 384 K.

DOI: 10.1021/jacs.5b02373
J. Am. Chem. Soc. 2015, 137, 6335−6349

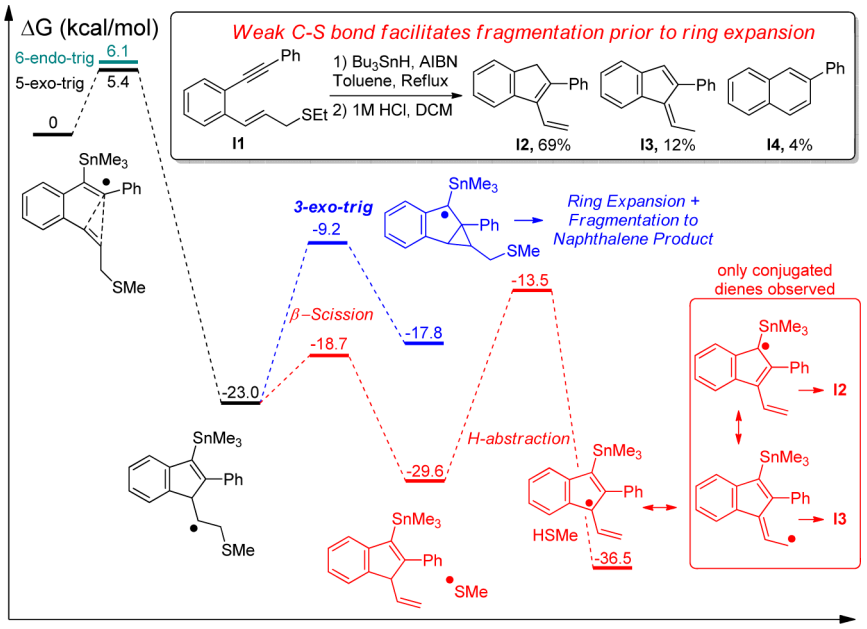

Figure 13. Alternate reactivity and calculated free energy profile (UM062X/LanL2DZ) for thio-substituted enynes. ΔG values, in kcal/mol, are calculated at 384 K. The new "radical clock" pathway based on the β-scission of a weak C−S bond is shown in red.

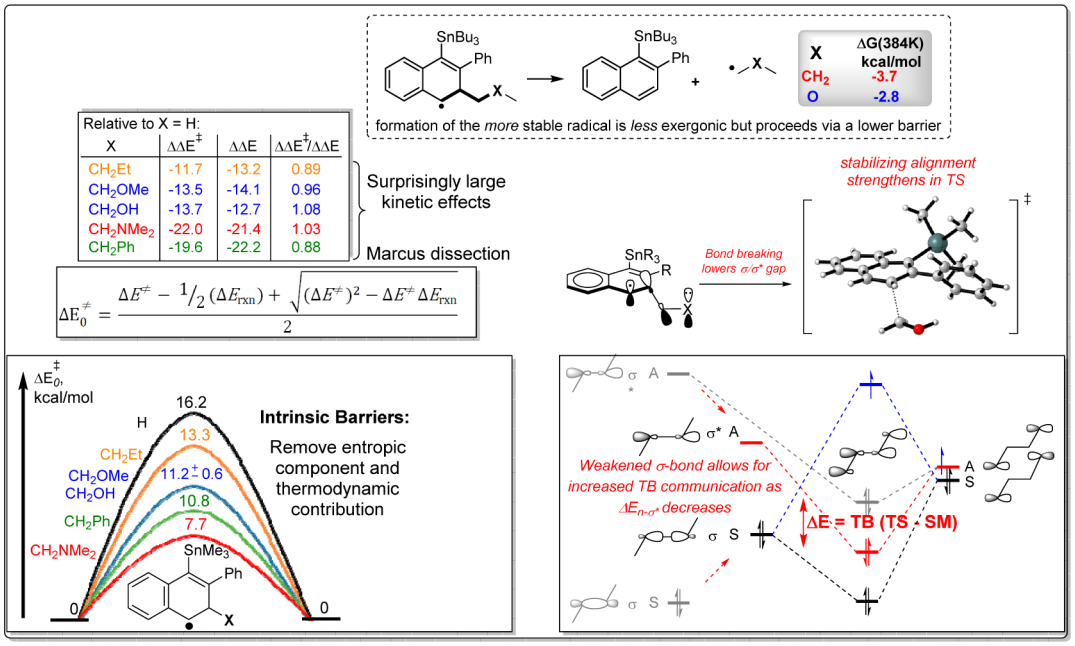

Figure 14. Top: Fragmentation paradox formation of the more stable radical is calculated as less exergonic, indicating a remote stabilizing effect arising in the benzylic radical. Energies in kcal/mol; ΔG values are calculated at 384 K using the UM06-2X/LanL2DZ level of theory. Bottom: Stereoelectronics of the fragmentation viewed through the prism of Marcus theory.[58,59] The top inset summarizes differences in reaction and activation free energies imposed by the substituents. The bottom inset shows intrinsic reaction barriers for the fragmentation. Electronic coupling between nonbonding orbitals in 1,4-diradicals and β-heteroatom-substituted radicals strengthens in the TS, facilitating C−C bond fragmentation. Additional stabilization due to TB coupling through the breaking bridging bond is shown as ΔE (red). σ and σ^* energies in the starting radical are shown in gray. Left: Optimized geometry for the fragmentation TS (X = CH_2OH). Right: Orbital alignment with the σ^* of the bridge facilitates TB coupling between the nonbonding orbitals, leading to the fragmentation. For a more detailed discussion of these effects, see ref 14.

conjugation (as it does for Ph-substituted alkenes), the difference in the activation barriers between the two pathways remained significant (e.g., $\Delta\Delta G^{\ddagger} \sim 2.6$ kcal/mol). This is not surprising because intramolecular radical attack at π-bonds intrinsically favors the exo path,[49] unless special factors such as steric or polar effects can overweigh this intrinsic preference.[50−52]

Once highly exothermic (~20 kcal) and essentially irreversible 5-exo-trig cyclization takes place, the alkyl radical adduct is flexible enough to allow intramolecular rearrangement that ultimately affords the formal 6-endo product (Figure 12). The key step in this rearrangement is the 3-exo-trig attack at the double bond of indene to provide a radical that, albeit strained, enjoys both benzylic and α-Sn stabilization. The

DOI: 10.1021/jacs.5b02373
J. Am. Chem. Soc. 2015, 137, 6335−6349

subsequent C−C bond fragmentation releases strain and relocates the radical center to the other benzylic position. The final benzylic radical is ∼30 kcal/mol more stable than the vinyl radical at the entry point of the cascade. At the final step, aromatizing β-C−C bond scission yields the Sn-substituted naphthalene. Although this mechanism involves a relatively complex rearrangement, it can provide the final product in >80% yield.

Interestingly, both 5-exo and 6-endo-trig cyclizations have lower barriers for R = CH_2SEt, and the calculated difference in the two barriers decreased to only 0.7 kcal/mol (Figure 13). In good agreement with these computational results, a small amount of the 6-endo product was observed in the reaction, indicating that the presence of a β-C−S bond at the alkene terminus facilitated 6-endo cyclization.

Conceptual Implications: The Role of Aromaticity and Through-Bond Interactions in the C−C Bond Fragmentation Step. Furthermore, computational analysis of the reaction led to intriguing theoretical implications regarding the role of electronic effects. Although radical fragmentations provide a valuable option for the termination of cascade transformations,[53] both thermodynamics and kinetics of this process need to be optimized in order to break unstrained C−C bonds under relatively mild conditions.[54] The unusually facile homolytic cleavage of an unstrained C−C bond is assisted by aromatic stabilization gained in the naphthalene product. In order to investigate the evolution of aromaticity throughout the reactions, NICS values were calculated throughout the reaction coordinate (see Figure S7 in Supporting Information). NICS values were calculated in the plane of the forming aromatic ring, 1 Å above the plane and 1 Å below. NICS(1) values, a better measure of π-aromaticity than NICS(0),[55] show the development of aromaticity along the reaction coordinate, going from nonaromatic (NICS(1) = −2−0 ppm) reactant to aromatic (NICS(1) ∼ 9.5 ppm) product. Thus, this process provides an interesting addition to the family of aromaticity-driven organic reactions.[56]

The facilitating effect of aromaticity is well-established and has many precedents. However, the influence of a remote lone pair (positioned at the δ-atom) at the radical reactivity is novel and conceptually interesting. The significant effect observed in the computational analysis of the C−C bond fragmentation step points to the existence of a new electronic interaction of potentially broad importance for radical chemistry. Free energies (ΔG) for the final C−C bond fragmentation yielding the aromatic naphthalene product are negative due to the combination of radical stabilization and favorable entropic contribution. Somewhat paradoxically, fragmentation leading to the formation of the *more* stable α-oxy radical (OCH_2Me, Figure 10) is *less* exothermic than the analogous fragmentation of the propyl radical (Figure 14). We suggested earlier that this surprising observation can be explained by the presence of a stabilizing through-bond interaction[57] between the benzylic radical and the lone pair at the δ-position.[14] The role of TB coupling between two nonbonding orbitals populated with three electrons is not commonly recognized; however, as shown in Figure 9 (top), the calculated fragmentation exergonicities for O-containing substrates (CH_2OMe/CH_2OH) are lower than that for propyl-substituted substrate, indicating a stabilization of the benzylic radical containing a β-C−X bond.

Furthermore, the odd-electron TB communication between the radical and the lone pair through the σ-bridge serves as a stereoelectronic conduit for kinetic acceleration of the bond scission because this electronic effect is increased at the transition state. Along the reaction path, the calculated molecular geometry in the CCOH moiety changes to adopt the coplanar arrangement between the radical center and the p-type lone pair on oxygen. The increase in TB interaction through stretched bonds can be understood from the second-order perturbation energies provided by NBO analysis. During fragmentation, the energy of the σ^*-antibonding orbital is lowered, decreasing the ΔE_{ij} term for a stabilizing interaction with the antisymmetric combination of nonbonding orbitals (i.e., the radical and lone pair). In addition, as the fragmentation progresses, the ∼sp^3 σ-bond is transformed into two p-orbitals (one π-bonded in naphthalene and the other in a 2c-3e "half-bond"), increasing overlap between interacting orbitals (Figure 14, bottom right). Together these interactions are responsible for selective TS stabilization for the fragmentation process.[60] Additional discussion of this interesting phenomenon is provided in the Supporting Information.

Although the importance of such three-electron TB interactions has not been previously recognized in radical chemistry, similar effects are involved in the fragmentation of radical cations reported earlier by the groups of Whitten[61] and Kutateladze.[62] The latter group also utilized this chemistry creatively in bioanalytical applications (Figure 15).[63] Our work provides an approach to study these intriguing orbital effects in neutral compounds.

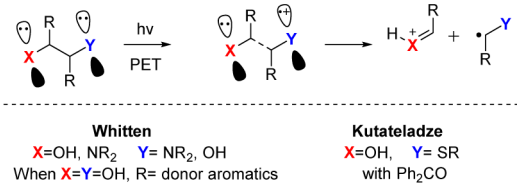

Figure 15. Selected examples of cationic fragmentations where three-electron through-bond interactions are likely to play an accelerating role.

Practical Applications: Access to Extended Polyaromatics. For convenience, we usually remove the Bu_3Sn moiety by protodestannylation of the reaction mixtures prior to purification. However, the Sn moiety in the indene and naphthalene products can be retained and utilized as a useful functionality for further synthetic transformations. In particular, Stille coupling and iodination of the α-Sn-substituted naphthalene confirmed the direction of tin attack and presented a synthetic advantage for facile functionalization of naphthalene cores. Both approaches provided highly substituted naphthalene derivatives that are otherwise difficult to prepare from the parent aromatic core, as shown in Scheme 9.

As noted above, changing the alkyne substituent in simple enynes, from benzene to naphthalene or anthracene, decreases the product yield. We attribute this decrease to an increase in steric congestion during the intramolecular attack of the vinyl radical on the alkene (Figure 11, compounds **K33** and **K34**). The stabilizing effect of conjugating substituents for the unproductive Bu_3Sn attack at the external alkyne (and, possibly, alkene) positions poses limitations that are illustrated by unsuccessful attempts to directly access triphenylene derivatives from the cyclization of enyne **P7** shown in Scheme 10.

To test the validity of the above assumption, we moved conjugating substituents to the outside aryl group where they

DOI: 10.1021/jacs.5b02373
J. Am. Chem. Soc. 2015, 137, 6335−6349

Scheme 9. Use of thre Bu_3Sn Group as a Functional Handle for the Preparation of More Substituted Naphthalene Building Blocks[a]

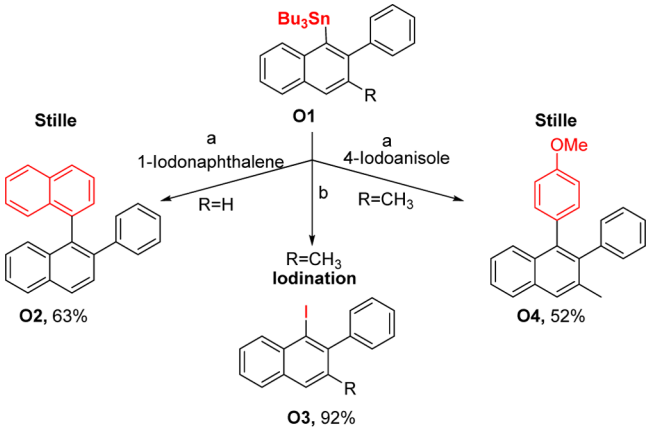

[a]Conditions: (a) 0.1 equiv of $Pd(PPh_3)_4$, 5 equiv of CuCl, 6 equiv of LiBr, DMF, 100 °C, 12 h; (b) I_2, DCM, 8 h, rt.

Scheme 10. Conjugating Substituents at the Core Interfere with Cyclization but the Same Substituents at the Periphery Effectively Participate in the Reaction[a]

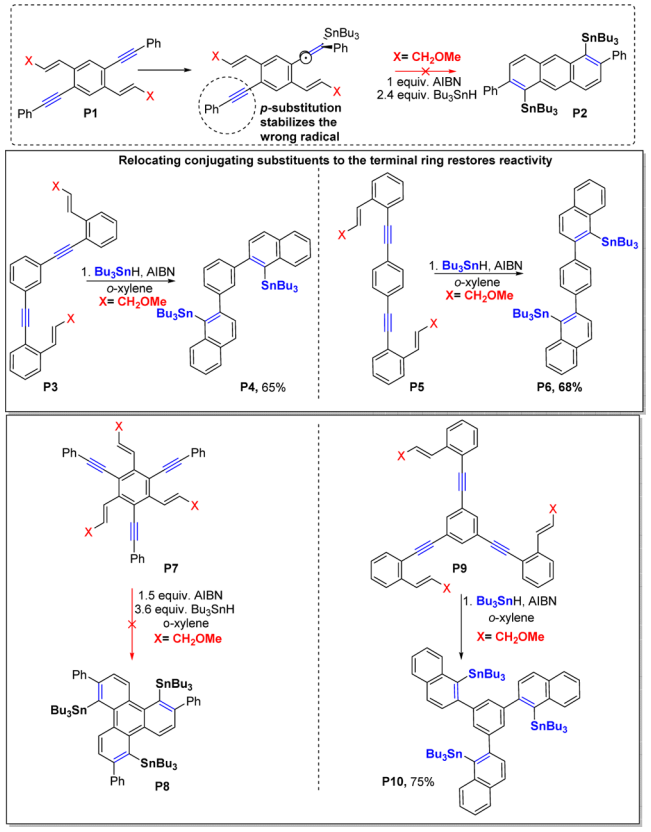

[a]Substitution at the cores is likely to make the substrates too crowded for successful cyclization using the bulky Bu_3Sn radical.

would stabilize the *productive* radicals. To our delight, we found that, with this structural change, the reaction successfully gives bis- and trisnaphthalene-substituted biphenyl compounds **P4** and **P6** in excellent yield (Scheme 10). The success of the cascade and selectivity of the transformation was confirmed by X-ray analysis (see Supporting Information). The overall efficiency of >75% is remarkable considering that *nine* bonds were formed and *six* bonds were broken in the process of this cascade that involves the cyclization/expansion/fragmentation sequence at each of the three enyne functionalities.

Furthermore, such products can serve as a convenient launching point for the preparation of extended polyaromatics. For example, the successful iodination of the Sn-substituted 1,3,5-tris(naphthyl)benzene structure **P10** creates a versatile scaffold for iterative expansion into larger derivatives. Suzuki coupling with (4-pentylphenyl)boronic acid, phenyl boronic acid, and bromophenyl boronic acid yielded **Q2**, **Q4**, and **Q5** in 92, 95, and 30% yield, respectively. Alternatively, Sonogashira coupling with phenylacetylene gave the trialkynyl product **Q3** in 86% (Scheme 11).

Photophysical Properties of Selected Extended Compounds. The photophysical properties for select compounds (**O2**, **Q2**, **Q3**, and **Q4**) were recorded in dichloromethane, and the results are summarized in Table S1 in the Supporting Information. Representative spectra for emission and absorption from 5 μM solutions of the compound are shown in Figure 16. The low-energy absorption onset (~330 nm) and absorption maxima (~290 nm) for **O2**, **Q2**, and **Q4** are similar. This feature can presumably be attributed to $\pi-\pi^*$ transition of the naphthyl moiety. In contrast, compound **Q3** exhibits a ~50 nm red shift in absorption features relative to **O2**, **Q2**, and **Q4**. This red shift is expected given the extended conjugation of the phenylacetylene functionalization of the naphthyl groups in **Q3** relative to the other complexes. Similar to that observed with absorption, emission energies trend in the order of **O2** ≈ **Q2** ≈ **Q4** > **Q3** (Figure S1).

The luminescent quantum yields (Φ) for **Q3** and **O2**, measured by using an integrating sphere, were found to be 0.303 and 0.0194, respectively. Due to their relatively low emission intensities, the quantum yields for **Q2** (0.0014) and **Q4** (0.0018) were obtained relative to **O2**. Despite having the shortest lifetime, 1.75 ns, **Q3** exhibits an order of magnitude higher emission quantum yield than the other complexes. Given the similarity in nonradiative decay rates (k_{nr} = 1.78–3.98 × 10^8 s^{-1}), the increased emission yield can be attributed to a radiative rate constant (k_r) that is significantly higher for **Q3** (17.3 × 10^7 s^{-1}) and moderately higher for **O2** (0.35 × 10^7 s^{-1}) relative to **Q2** (0.03 × 10^7 s^{-1}) and **Q4** (0.04 × 10^7 s^{-1}). The origin of the increased radiative rates for **Q3** is not currently understood.

In addition to the high-energy absorption feature at ~350 nm for **Q2** and **Q4**, there is a second low-energy emission band between 440 and 580 nm (Figure 16b,d). The excitation spectra for both emission features resemble the absorption spectra for the complex, indicating that it is not simply an emission impurity. The absorption features of **Q2** and **Q4** were consistent at both high and low concentrations, suggesting that there is minimal ground state aggregation in these complexes. However, in the emission spectra, the ratio of the peak intensities (I_{370nm}/I_{500nm}) increases steadily with dilution (Figures S2 and S3), indicating that the low-energy emission feature may be due to excimer formation for **Q2** and **Q4**, even in dilute solutions.

■ CONCLUSIONS

This work presents a full experimental and theoretical study of the first radical enyne cascade in which chemo- and regioselective interaction of the triple bond with Bu_3Sn radicals

DOI: 10.1021/jacs.5b02373
J. Am. Chem. Soc. 2015, 137, 6335–6349

Scheme 11. Utility of the Sn Functional Handle Is Demonstrated by Iodination and Subsequent Extension of the Trinaphthalene Aromatic Core with Suzuki and Sonogashira Couplings To Form Large Functionalized Polyaromatics

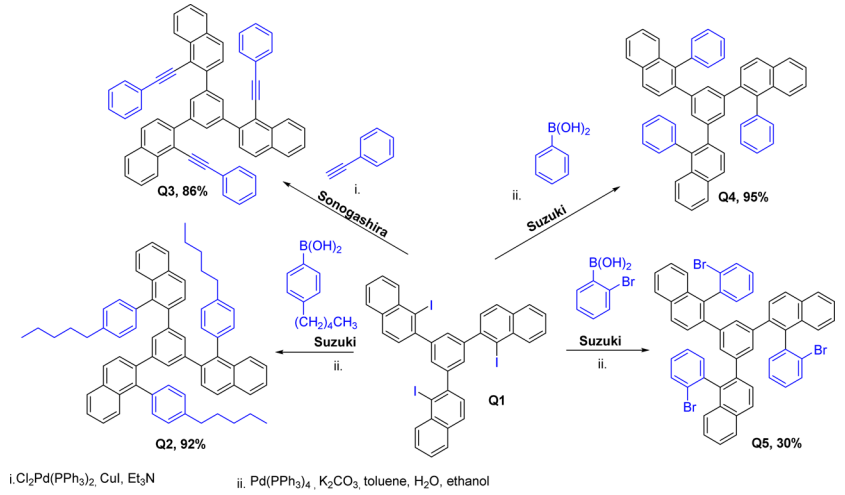

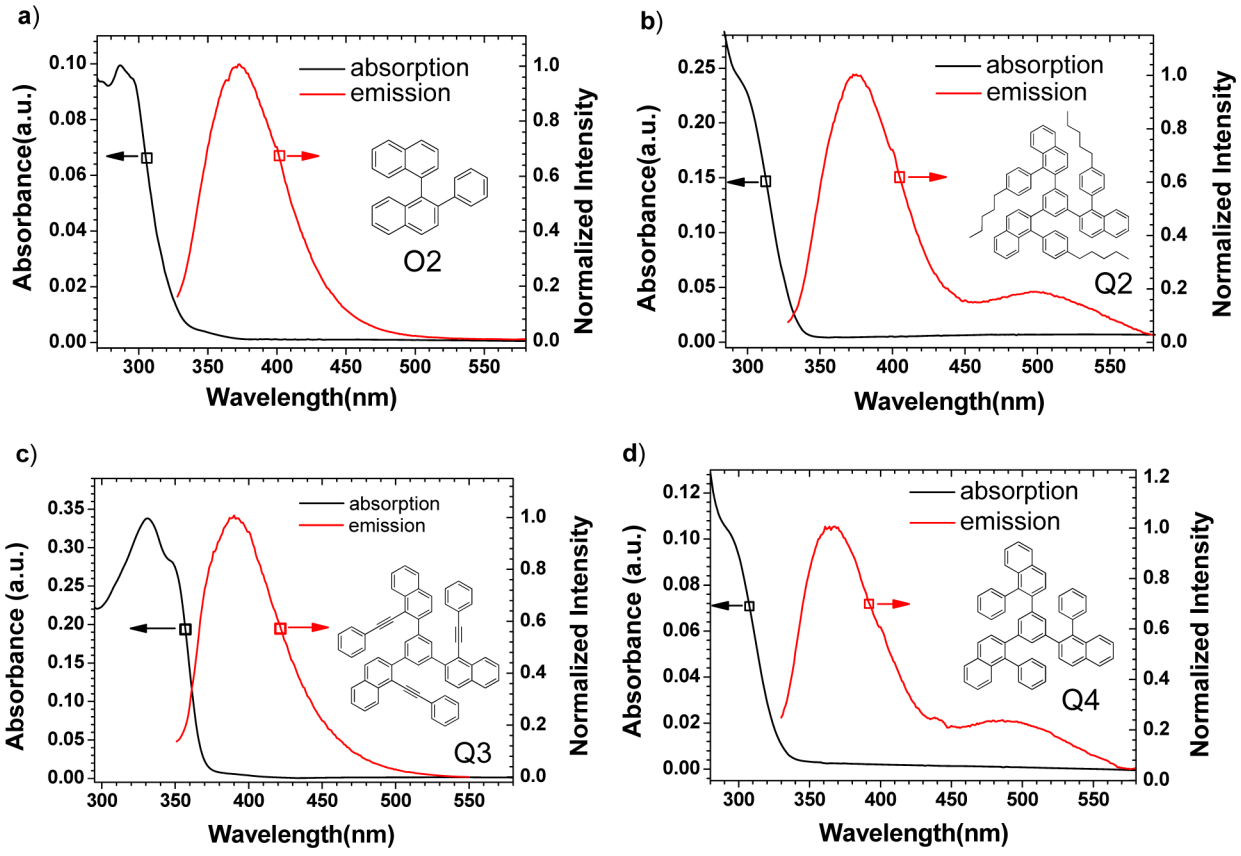

Figure 16. Room temperature absorption and normalized emission spectra of compounds **O2** (a), **Q2** (b), **Q3** (c), and **Q4** (d) in dichloromethane (5×10^{-6} M).

originates from a conceptually novel source and propagates in an unprecedented sequence of steps that renders alkenes synthetic equivalents of alkynes. The previously inaccessible 6-endo-dig products are obtained by coupling cyclization/rearrangement cascade with an aromatizing C−C bond fragmentation. The net result is a convenient transformation of readily available enyne reactants to α-Sn-substituted naphthalenes that can be used as a launching platform for the preparation of extended distorted polyaromatics. Every step in the multistep cascade provides fundamental insights in the new ways to control radical transformations. In particular, the remarkable chemo- and regioselectivity of the initial radical attack originate from the combination of dynamic covalent chemistry with kinetic self-sorting. Furthermore, we have identified a new 1,2-stannyl shift as a low-barrier mechanism for the conversion of an unproductive vinyl radical to the radical adduct which can undergo fast 5-exo-trig closure (serving as kinetic self-sorting). We have also identified substitution patterns that can *selectively* direct the initially formed cyclic radical to react further in one of the following

DOI: 10.1021/jacs.5b02373
J. Am. Chem. Soc. 2015, 137, 6335−6349

three ways: H-abstraction, β-scission, or ring expansion. Unlike the analogous radical that would be formed from a 5-exo-dig closure of an enediyne, the 5-exo-trig product originating from the *enyne* is sufficiently flexible to undergo homoallylic ring expansion to the formal 6-endo product. In the overall sequence, the alkene moiety of enynes serves as a synthetic alkyne equivalent because this radical sequence "self-terminates" via aromatizing C−C bond cleavage. The key C−C bond fragmentation is assisted by a new electronic effect in radical chemistry, the three-electron through-bonding interaction. This interaction provides a conduit for selective transition state stabilization in the fragmentation process.

■ ASSOCIATED CONTENT

Supporting Information

Full experimental details, ^{1}H NMR, ^{13}C NMR, NMR spectra for all of the prepared compounds, X-ray crystallographic data for selected products, and computational details for all calculated structures. The Supporting Information is available free of charge on the ACS Publications website at DOI: 10.1021/jacs.5b02373.

■ AUTHOR INFORMATION

Corresponding Author

*alabugin@chem.fsu.edu

Author Contributions

†These authors contributed equally.

Notes

The authors declare no competing financial interest.

■ ACKNOWLEDGMENTS

The fundamental and synthetic aspects of this study were supported by the National Science Foundation (Grants CHE-1152491 and CHE-1213578).

■ REFERENCES

(1) (a) Müllen, K. *ACS Nano* **2014**, *8*, 6531. (b) Türp, D.; Nguyen, T. T. T.; Baumgarten, M.; Müllen, K. *New J. Chem.* **2012**, *36*, 282. (c) Scholl, R.; Seer, C.; Weitzenböck, R. *Chem. Ber.* **1910**, *43*, 2202. (d) Clar, E. *Polycyclic Hydrocarbons*; Academic Press: London, 1964. (e) Ito, S.; Takahashi, K.; Nozaki, K. *J. Am. Chem. Soc.* **2014**, *136*, 7547. (f) Blake, A. J.; Cooke, P. A.; Doyle, K. J.; Gair, S.; Simpkins, N. S. *Tetrahedron Lett.* **1998**, *39*, 9093. (g) Ball, M.; Zhong, Y.; Wu, Y.; Schenck, C.; Ng, F.; Steigerwald, M.; Xiao, S.; Nuckolls, C. *Acc. Chem. Res.* **2014**, *48*, 267. (h) Anthony, J. *Chem. Rev.* **2006**, *106*, 5028. (i) Abdurakhmanova, N.; Amsharov, N.; Stepanow, S.; Jansen, M.; Kern, K.; Amsharov, K. *Carbon* **2014**, *77*, 1187.

(2) Selected examples (a) Goldfinger, M. B.; Crawford, K. B.; Swager, T. M. *J. Am. Chem. Soc.* **1997**, *119*, 4578. (b) Feng, X.; Pisula, W.; Müllen, K. *Pure Appl. Chem.* **2009**, *81*, 2203. (c) Scott, L. T.; Jackson, E. A.; Zhang, Q.; Steinberg, B. D.; Bancu, M.; Li, B. *J. Am. Chem. Soc.* **2012**, *134*, 107. (d) Luo, L.; Resch, D.; Wilhelm, C.; Young, C. N.; Halada, G. P.; Gambino, R. J.; Grey, C. P.; Goroff, N. S. *J. Am. Chem. Soc.* **2011**, *133*, 19274. (e) Riss, A.; Wickenburg, S.; Gorman, P.; Tan, L. Z.; Tsai, H.-Z.; de Oteyza, D. G.; Chen, Y.-C.; Bradley, A. J.; Ugeda, M. M.; Etkin, G.; Louie, S. G.; Fischer, F. R.; Crommie, M. F. *Nano Lett.* **2014**, *14*, 2251. (f) Hein, S. J.; Arslan, H.; Keresztes, I.; Dichtel, W. R. *Org. Lett.* **2014**, *16*, 4416.

(3) (a) Matzger, A. J.; Vollhardt, K. P. C. *Chem. Commun.* **1997**, *15*, 1415. (b) Cataldo, F. *Carbon* **2004**, *42*, 129. (c) Diederich, F.; Kivala, M. *Adv. Mater.* **2010**, *22*, 803. (d) Chernick, E.; Tykwinski, R. *J. Phys. Org. Chem.* **2013**, *26*, 742. Intermolecular initiation (e) Alabugin, I. V.; Gilmore, K.; Patil, S.; Manoharan, M.; Kovalenko, S. V.; Clark, R. J.; Ghiviriga, I. *J. Am. Chem. Soc.* **2008**, *130*, 11535. Intramolecular initiation: (f) Byers, P. M.; Alabugin, I. V. *J. Am. Chem. Soc.* **2012**, *134*, 9609. (g) Pati, K.; Hughes, A. M.; Phan, H.; Alabugin, I. V. *Chem.—Eur. J.* **2014**, *20*, 390.

(4) Narita, A.; Feng, X.; Hernandez, Y.; Jensen, S. A.; Bonn, M.; Yang, H.; Verzhbitskiy, I. A.; Casiraghi, C.; Hansen, M. R.; Koch, A. H. R.; Fytas, G.; Ivasenko, O.; Li, B.; Mali, K. S.; Balandina, T.; Mahesh, S.; Feyter, S. D.; Müllen, K. *Nat. Chem.* **2014**, *6*, 126.

(5) Pati, K.; dos Passos Gomes, G.; Harris, T.; Hughes, A.; Phan, H.; Banerjee, T.; Hanson, K.; Alabugin, I. V. *J. Am. Chem. Soc.* **2015**, *137*, 1165.

(6) However, the desired 6-endo selectivity can be achieved via metal catalysis in conjunction with the "LUMO Umpolung" approach: (a) Byers, P. M.; Rashid, J. I.; Mohamed, R. K.; Alabugin, I. V. *Org. Lett.* **2012**, *14*, 6032. (b) Alabugin, I. V.; Gilmore, K. *Chem. Commun.* **2013**, *49*, 11246. (c) Zhang, J.; Yang, C.-G.; He, C. *J. Am. Chem. Soc.* **2006**, *128*, 1798. (d) Hashmi, A. S. K.; Braun, I.; Rudolph, M.; Rominger, F. *Organometallics* **2012**, *31*, 644.

(7) General discussion of exoselectivity in radical reactions: (a) Beckwith, A. L. J. *Tetrahedron* **1981**, *37*, 3073. (b) Beckwith, A. L. J.; Schiesser, C. H. *Tetrahedron* **1985**, *41*, 3925. General discussion on selectivity of alkyne cyclizations: (c) Gilmore, K.; Alabugin, I. V. *Chem. Rev.* **2011**, *111*, 6513. (d) Alabugin, I. V.; Gilmore, K.; Manoharan, M. *J. Am. Chem. Soc.* **2011**, *133*, 12608. (e) 5-exo/6-endo competition in conjugated systems: Alabugin, I. V.; Manoharan, M. *J. Am. Chem. Soc.* **2005**, *127*, 12583.

(8) (a) Rainier, J. D.; Kennedy, A. R. *J. Org. Chem.* **2000**, *65*, 6213. (b) Rainier, J. D.; Kennedy, A. R.; Chase, E. *Tetrahedron Lett.* **1999**, *40*, 6325. (c) Bharucha, K. N.; Marsh, R. M.; Minto, R. E.; Bergman, R. G. *J. Am. Chem. Soc.* **1992**, *114*, 3120. (d) Matzger, A. J.; Vollhardt, K. P. C. *Chem. Commun.* **1997**, 1415. (e) Lin, C.-F.; Wu, M.-J. *J. Org. Chem.* **1997**, *62*, 4546. (f) Wu, H. J.; Lin, C. F.; Lee, J. L.; Lu, W. D.; Lee, C. Y.; Chen, C. C.; Wu, M. J. *Tetrahedron* **2004**, *60*, 3927.

(9) (a) Kovalenko, S. V.; Peabody, S.; Manoharan, M.; Clark, R. J.; Alabugin, I. V. *Org. Lett.* **2004**, *6*, 2457. (b) Peabody, S.; Breiner, B.; Kovalenko, S. V.; Patil, S.; Alabugin, I. V. *Org. Biomol. Chem.* **2005**, *3*, 218.

(10) Nagarjuna, G.; Ren, Y.; Moore, J. S. *Tetrahedron Lett.* **2015**, DOI: 10.1016/j.tetlet.2015.01.011.

(11) (a) Newcomb, M.; Glenn, A. G.; Williams, W. G. *J. Org. Chem.* **1989**, *54*, 2675. (b) Stork, G.; Mook, R. *Tetrahedron Lett.* **1986**, *27*, 4529.

(12) (a) Beckwith, A. L. J.; O'Shea, D. M. *Tetrahedron Lett.* **1986**, *27*, 4525. (b) Beckwith, A. L. J.; Bowry, V. W. *J. Org. Chem.* **1989**, *54*, 2681.

(13) (a) Mondal, S.; Mohamed, R. K.; Manoharan, M.; Phan, H.; Alabugin, I. V. *Org. Lett.* **2013**, *15*, 5650. (b) Mondal, S.; Gold, B.; Mohamed, R. K.; Phan, H.; Alabugin, I. V. *J. Org. Chem.* **2014**, *79*, 7491.

(14) Mondal, S.; Gold, B.; Mohamed, R. K.; Alabugin, I. V. *Chem.—Eur. J.* **2014**, *20*, 8664.

(15) Frisch, M. J.; Trucks, G. W.; Schlegel, H. B.; Scuseria, G. E.; Robb, M. A.; Cheeseman, J. R.; Scalmani, G.; Barone, V.; Mennucci, B.; Petersson, G. A.; Nakatsuji, H.; Caricato, M.; Li, X.; Hratchian, H. P.; Izmaylov, A. F.; Bloino, J.; Zheng, G.; Sonnenberg, J. L.; Hada, M.; Ehara, M.; Toyota, K.; Fukuda, R.; Hasegawa, J.; Ishida, M.; Nakajima, T.; Honda, Y.; Kitao, O.; Nakai, H.; Vreven, T.; Montgomery, J. A., Jr.; Peralta, J. E.; Ogliaro, F.; Bearpark, M.; Heyd, J. J.; Brothers, E.; Kudin, K. N.; Staroverov, V. N.; Kobayashi, R.; Normand, J.; Raghavachari, K.; Rendell, A.; Burant, J. C.; Iyengar, S. S.; Tomasi, J.; Cossi, M.; Rega, N.; Millam, M. J.; Klene, M.; Knox, J. E.; Cross, J. B.; Bakken, V.; Adamo, C.; Jaramillo, J.; Gomperts, R.; Stratmann, R. E.; Yazyev, O.; Austin, A. J.; Cammi, R.; Pomelli, C.; Ochterski, J. W.; Martin, R. L.; Morokuma, K.; Zakrzewski, V. G.; Voth, G. A.; Salvador, P.; Dannenberg, J. J.; Dapprich, S.; Daniels, A. D.; Farkas, Ö.; Foresman, J. B.; Ortiz, J. V.; Cioslowski, J.; Fox, D. J. *Gaussian 09*, revision C.01; Gaussian, Inc.: Wallingford, CT, 2009.

(16) (a) Zhao, Y.; Truhlar, D. G. *Theor. Chem. Acc.* **2008**, *120*, 215. (b) Zhao, Y.; Truhlar, D. G. *Acc. Chem. Res.* **2008**, *41*, 157.

(17) (a) Schleyer, P. v. R.; Maerker, C.; Dransfeld, A.; Jiao, H.; Hommes, J. v. E. *J. Am. Chem. Soc.* **1996**, *118*, 6317. (b) Mills, N. S. *J.*

DOI: 10.1021/jacs.5b02373
J. Am. Chem. Soc. 2015, 137, 6335−6349

Am. Chem. Soc. **1999**, *121*, 11690. (c) Levy, A.; Rakowitz, A.; Mills, N. S. *J. Org. Chem.* **2003**, *68*, 3990. (d) Mills, N. S. *J. Org. Chem.* **2002**, *67*, 7029. (e) Alkorta, I.; Rozas, I.; Elguero, J. *Tetrahedron* **2001**, *57*, 6043.
(18) (a) Wolinski, K.; Hinton, J. F.; Pulay, P. *J. Am. Chem. Soc.* **1990**, *112*, 8251. (b) Dichfield, R. *Mol. Phys.* **1974**, *27*, 789.
(19) Andrienko, G. A. *ChemCraft*; Bluesnap, Inc.: Waltham, MA, http://www.chemcraftprog.com.
(20) Legault, C. Y. *CYLview*, 1.0b; Université de Sherbrooke: Quebec, Canada, 2009; http://www.cylview.org.
(21) (a) Reed, A. E.; Weinhold, F. *J. Chem. Phys.* **1985**, *83*, 1736. (b) Reed, A. E.; Weinhold, F. *Isr. J. Chem.* **1991**, *31*, 277. (c) Reed, A. E.; Curtiss, L. A.; Weinhold, F. *Chem. Rev.* **1988**, *88*, 899. (d) Weinhold, F. In *Encyclopedia of Computational Chemistry*; Schleyer, P. v. R., Ed.; Wiley: New York, 1998; Vol. 3, p 1792.
(22) Baguley, P. A.; Walton, J. C. *Angew. Chem., Int. Ed.* **1998**, *37*, 3072.
(23) (a) Kuivila, H. G. *Acc. Chem. Res.* **1968**, *1*, 299. (b) Giese, B. *Radicals in Organic Synthesis: Formation of Carbon−Carbon Bonds*; Pergamon Press: Oxford, UK, 1986. (c) Neumann, W. P. *Synthesis* **1987**, 665. (d) Curran, D. P. *Synthesis* **1988**, 417. (e) Curran, D. P. *Synthesis* **1988**, 479. (f) Curran, D. P. In *Comprehensive Organic Synthesis*; Trost, B. M., Fleming, I., Eds.; Pergamon: Oxford, UK, 1991; Vol. 4, p 715. (g) Motherwell, W.; Crich, D. In *Free Radical Chain Reactions in Organic Synthesis*; Academic Press: London, 1992; p 259. (h) Rajanbabu, T. V. In *Encyclopedia of Reagents for Organic Synthesis*; Paquette, L., Ed.; Wiley: New York, 1995; Vol. 7, p 5016.
(24) Wille, U. *Chem. Rev.* **2013**, *113*, 813.
(25) Nozaki, K.; Oshima, K.; Utimoto, K. *Tetrahedron* **1989**, *45*, 923.
(26) Gómez, A. M.; Uriel, C.; Company, M. D.; López, J. C. *Eur. J. Org. Chem.* **2011**, 7116.
(27) (a) Stork, G.; Mook, R., Jr. *Tetrahedron Lett.* **1986**, *27*, 4529. (b) Stork, G.; Mook, R., Jr. *J. Am. Chem. Soc.* **1987**, *109*, 2829. (c) Stork, G.; Baine, N. H. *J. Am. Chem. Soc.* **1982**, *104*, 2321.
(28) However, the same experiment with *cis*-stilbene showed that, along with addition to the alkyne, significant isomerization of the *cis*-stilbene into *trans*-stilbene took place under radical initiation conditions. These experiments suggest that reversible addition to the alkenes may occur as well but remains invisible. We plan to investigate this phenomenon in detail in future studies.
(29) This concept provides an interesting counterpart to "pools of cations", an elegant concept introduced by Yoshida and co-workers: Okajima, M.; Suga, S.; Itami, K.; Yoshida, J.-i. *J. Am. Chem. Soc.* **2005**, *127*, 6930.
(30) Ji, Q.; Lirag, R. C.; Miljanić, O. Š. *Chem. Soc. Rev.* **2014**, *43*, 1873.
(31) Rowan, S. J.; Cantrill, S. J.; Cousins, G. R. L.; Sanders, J. K. M.; Stoddart, J. F. *Angew. Chem., Int. Ed.* **2002**, *41*, 898.
(32) Jin, Y.; Wang, Q.; Taynton, P.; Zhang, W. *Acc. Chem. Res.* **2014**, *47*, 1575.
(33) For such strong interactions, energies are sensitive to orbital overlap. When the vicinal acceptor center is separated from the donor by a double bond, the shorter distance between the interacting groups enhances orbital overlap. See: Alabugin, I. V.; Zeidan, T. A. *J. Am. Chem. Soc.* **2002**, *124*, 3175.
(34) Anslyn, E. V.; Dougherty, D. A. *Modern Physical Organic Chemistry*; University Science Books: Sausalito, CA, 2006.
(35) For examples of TS stabilization in alkyne reactions, see: (a) Gold, B.; Batsomboon, P.; Dudley, G. B.; Alabugin, I. V. *J. Org. Chem.* **2014**, *79*, 6221. (b) Gold, B.; Dudley, G. B.; Alabugin, I. V. *J. Am. Chem. Soc.* **2013**, *135*, 1558.
(36) Alabugin, I. V.; Bresch, S.; Manoharan, M. *J. Phys. Chem. A* **2014**, *118*, 3663.
(37) Alabugin, I. V.; Bresch, S.; dos Passos Gomes, G. *J. Phys. Org. Chem.* **2015**, *28*, 147.
(38) (a) McMaster, A. D.; Stobart, S. R. *J. Am. Chem. Soc.* **1982**, *104*, 2109. (b) Atwood, J. L.; McMaster, A. D.; Robin, R. D.; Stobart, S. R. *Organometallics* **1984**, *3*, 1500.
(39) (a) Gridnev, I. D.; Schreiner, P. R.; Gurskii, M. E.; Bubnov, Y. N.; Krasavin, A. O.; Mstislavski, V. I. *Chem. Commun.* **1998**, 2507. (b) Hails, M. J.; Mann, B. E.; Spencer, C. M. *J. Chem. Soc., Dalton Trans.* **1983**, 729.
(40) Gridnev, I. D.; Schreiner, P. R.; Tok, O. L.; Bubnov, Y. N. *Chem.—Eur. J.* **1999**, *5*, 2828.
(41) Nori-Shargh, D.; Roohi, F.; Deyhimi, F.; Naeem-Abyaneh, R. *J. Mol. Struct.* **2006**, *763*, 21.
(42) Alabugin, I. V.; Manoharan, M.; Breiner, B.; Lewis, F. D. *J. Am. Chem. Soc.* **2003**, *125*, 9329.
(43) Lambert, J. B.; Wang, G.; Teramura, D. H. *J. Org. Chem.* **1988**, *53*, 5422.
(44) (a) Wille, U.; Plath, C. *Liebigs Ann./Recl.* **1997**, 111. (b) Jargstorff, C.; Wille, U. *Eur. J. Org. Chem.* **2003**, 3173. (c) Wille, U. *Org. Lett.* **2000**, *2*, 3485.
(45) (a) Wille, U. *J. Am. Chem. Soc.* **2002**, *124*, 14. (b) Tan, K. J.; White, J. M.; Wille, U. *Eur. J. Org. Chem.* **2010**, 4902.
(46) Alabugin, I. V.; Gilmore, K.; Peterson, P. *Wiley Interdiscip. Rev.: Comput. Mol. Sci.* **2011**, *1*, 109.
(47) Alabugin, I. V.; Manoharan, M.; Zeidan, T. A. *J. Am. Chem. Soc.* **2003**, *125*, 14014.
(48) Wang, Z.; Zhang, L.; Zhang, F. *J. Phys. Chem. A* **2014**, *118*, 6741.
(49) (a) Beckwith, A. L. J.; Easton, C. J.; Serelis, A. K. *J. Chem. Soc., Chem. Commun.* **1980**, 482. (b) Spellmeyer, D. C.; Houk, K. N. *J. Org. Chem.* **1987**, *52*, 959.
(50) Alabugin, I. V.; Timokhin, V. I.; Abrams, J. N.; Manoharan, M.; Ghiviriga, I.; Abrams, R. *J. Am. Chem. Soc.* **2008**, *130*, 10984.
(51) Additional factors, such as transition state aromaticity, come into play for anionic endo-cyclizations. See: Gilmore, K.; Manoharan, M.; Wu, J.; Schleyer, P. v. R.; Alabugin, I. V. *J. Am. Chem. Soc.* **2012**, *134*, 10584.
(52) (a) Vasilevsky, S. F.; Mikhailovskaya, T. F.; Mamatyuk, V. I.; Bogdanchikov, G. A.; Manoharan, M.; Alabugin, I. V. *J. Org. Chem.* **2009**, *74*, 8106. (b) Vasilevsky, S. F.; Gold, B.; Mikhailovskaya, T. F.; Alabugin, I. V. *J. Phys. Org. Chem.* **2012**, *25*, 998.
(53) (a) Crich, D.; Bowers, A. *Org. Lett.* **2006**, *8*, 4327. (b) Baroudi, A.; Alicea, J.; Flack, P.; Kirincich, J.; Alabugin, I. V. *J. Org. Chem.* **2011**, *76*, 1521. (c) Baroudi, A.; Flack, P.; Alabugin, I. V. *Chem.—Eur. J.* **2010**, *16*, 12316. (d) Baroudi, A.; Alicea, J.; Alabugin, I. V. *Chem.—Eur. J.* **2010**, *16*, 7683. (e) Debien, L.; Zard, S. Z. *J. Am. Chem. Soc.* **2013**, *135*, 3808. (f) Heng, R.; Zard, S. Z. *Chem. Commun.* **2011**, *47*, 3296. (g) Kessabi, F. M.; Winkler, T.; Luft, J. A. R.; Houk, K. N. *Org. Lett.* **2008**, *10*, 2255. (h) Luft, J. A. R.; Winkler, T.; Murphy, F.; Kessabi, F. M.; Houk, K. N. *J. Org. Chem.* **2008**, *73*, 8175. (i) Quiclet-Sire, B.; Zard, S. Z. *Beilstein J. Org. Chem.* **2013**, *9*, 557. Similar transformation catalyzed by a radical (*S*)-adenosyl methionine (SAM) enzyme: (j) Mahanta, N.; Fedoseyenko, D.; Dairi, T.; Begley, T. P. *J. Am. Chem. Soc.* **2013**, *135*, 15318.
(54) For a recent review on C−C bond fragmentations, see: Drahl, M. A.; Manpadi, M.; Williams, L. J. *Angew. Chem., Int. Ed.* **2013**, *52*, 11222.
(55) Schleyer, P. v. R.; Maerker, C.; Dransfeld, A.; Jiao, H.; van Eikema Hommes, N. J. R. *J. Am. Chem. Soc.* **1996**, *118*, 6317.
(56) (a) Jones, R. R.; Bergman, R. G. *J. Am. Chem. Soc.* **1972**, *94*, 660. (b) Babinski, D. J.; Bao, X.; El Arba, M.; Chen, B.; Hrovat, D. A.; Borden, W. T.; Frantz, D. E. *J. Am. Chem. Soc.* **2012**, *134*, 16139. (c) Mohamed, R. K.; Peterson, P. W.; Alabugin, I. V. *Chem. Rev.* **2013**, *113*, 7089. (d) Peterson, P. W.; Mohamed, R. K.; Alabugin, I. V. *Eur. J. Org. Chem.* **2013**, 2505.
(57) (a) Hoffmann, R. *Acc. Chem. Res.* **1971**, *4*, 1. (b) Gleiter, R. *Angew. Chem.* **1974**, *86*, 77. (c) Gleiter, R. *Angew. Chem., Int. Ed. Engl.* **1974**, *13*, 696. (d) Paddon-Row, M. N. *Acc. Chem. Res.* **1982**, *15*, 245. (e) Abe, M. *Chem. Rev.* **2013**, *113*, 7011. (f) Gleiter, R.; Haberhauer, G. *Aromaticity and Other Conjugation Effects*; Wiley-VCH: Weinheim, Germany, 2012. (g) Alabugin, I. V.; Manoharan, M. *J. Phys. Chem. A* **2003**, *107*, 3363. (h) Yuan, L.; Sumpter, B. G.; Abboud, K. A.; Castellano, R. K. *New J. Chem.* **2008**, *32*, 1924. (i) Lampkins, A. J.; Li, Y.; Al Abbas, A.; Abboud, K. A.; Ghiviriga, I.; Castellano, R. K. *Chem.—Eur. J.* **2008**, *14*, 1452.
(58) (a) Marcus, R. A. *J. Chem. Phys.* **1956**, *24*, 966. (b) Marcus, R. A. *Annu. Rev. Phys. Chem.* **1964**, *15*, 155. (c) Marcus, R. A. *J. Phys. Chem.*

DOI: 10.1021/jacs.5b02373
J. Am. Chem. Soc. 2015, 137, 6335−6349

1968, *72*, 891. For alternative models, see also: (d) Evans, M. G.; Polanyi, M. *Trans. Faraday Soc.* **1938**, *34*, 11. (e) Koeppl, G. W.; Kresge, A. J. *J. Chem. Soc., Chem. Commun.* **1973**, 371.

(59) For the application of Marcus theory to radical reactions, see: (a) Alabugin, I. V.; Manoharan, M. *J. Am. Chem. Soc.* **2005**, *127*, 9534. For potential caveats, see: (b) Osuna, S.; Houk, K. N. *Chem.—Eur. J.* **2009**, *15*, 13219.

(60) For selected examples of TS stabilization for control of alkyne reactivity, see: Gold, B.; Shevchenko, N.; Bonus, N.; Dudley, G. B.; Alabugin, I. V. *J. Org. Chem.* **2012**, *77*, 75.

(61) (a) Ci, X.; Lee, L. Y. C.; Whitten, D. G. *J. Am. Chem. Soc.* **1987**, *109*, 2536. (b) Ci, X.; Whitten, D. G. *J. Am. Chem. Soc.* **1987**, *109*, 7215. (c) Ci, X.; Kellett, M. A.; Whitten, D. G. *J. Am. Chem. Soc.* **1991**, *113*, 3893. (d) Leon, J. W.; Whitten, D. G. *J. Am. Chem. Soc.* **1993**, *115*, 8038. (e) Baciocchi, E.; Bietti, M.; Putignani, L.; Steenken, S. *J. Am. Chem. Soc.* **1996**, *118*, 5952. (f) Chen, L.; Farahat, M. S.; Gan, H.; Farid, S.; Whitten, D. G. *J. Am. Chem. Soc.* **1995**, *117*, 6398. (g) Bergmark, W. R.; Whitten, D. G. *J. Am. Chem. Soc.* **1990**, *112*, 4042. (h) Gaillard, E. R.; Whitten, D. G. *Acc. Chem. Res.* **1996**, *29*, 292.

(62) (a) Li, Z.; Kutateladze, A. G. *J. Org. Chem.* **2003**, *68*, 8236. (b) Mitkin, O.; Wan, Y.; Kurchan, A.; Kutateladze, A. *Synthesis* **2001**, 1133. (c) Gustafson, T. P.; Kurchan, A. N.; Kutateladze, A. G. *Tetrahedron* **2006**, *62*, 6574. (d) Kurchan, A. N.; Kutateladze, A. G. *Org. Lett.* **2002**, *4*, 4129.

(63) Bioanalytical applications of C−C bond fragmentations: (a) Ezhov, R. N.; Metzel, G. A.; Mukhina, O. A.; Musselman, C. A.; Kutateladze, T. G.; Gustafson, T. P.; Kutateladze, A. G. *J. Photochem. Photobiol., A* **2014**, *290*, 101. (b) Gustafson, T. P.; Metzel, G. A.; Kutateladze, A. G. *Photochem. Photobiol. Sci.* **2012**, *11*, 564. (c) Gustafson, T. P.; Metzel, G. A.; Kutateladze, A. G. *Org. Biomol. Chem.* **2011**, *9*, 4752. (d) Kottani, R. R.; Majjigapu, J. R. R.; Kurchan, A. N.; Majjigapu, K.; Gustafson, T. P.; Kutateladze, A. G. *J. Am. Chem. Soc.* **2006**, *128*, 14794. (e) Kottani, R.; Valiulin, R. A.; Kutateladze, A. G. *Proc. Natl. Acad. Sci. U.S.A.* **2006**, *103*, 13917. (f) Majjigapu, J. R. R.; Kurchan, A. N.; Kottani, R.; Gustafson, T. P.; Kutateladze, A. G. *J. Am. Chem. Soc.* **2005**, *127*, 12458. (g) Wan, Y.; Angleson, J. K.; Kutateladze, A. G. *J. Am. Chem. Soc.* **2002**, *124*, 5610.

DOI: 10.1021/jacs.5b02373
J. Am. Chem. Soc. 2015, 137, 6335−6349